

## LIVE FUEL MOISTURE CONTENT AND IGNITION PROBABILITY IN THE IBERIAN PENINSULAR TERRITORY OF SPAIN

SARA JURDAO KNECHT<sup>1</sup>, MARTA YEBRA ÁLVAREZ<sup>2</sup>, AITOR BASTARRIKA IZAGIRRE<sup>3</sup> and EMILIO CHUVIECO SALINERO<sup>1</sup>

<sup>1</sup>Department of Geography and Geology, University of Alcalá.  
Calle Colegios 2, 28801. Alcalá de Henares. Spain.

[sara.jurdao@uah.es](mailto:sara.jurdao@uah.es), [emilio.chuvieco@uah.es](mailto:emilio.chuvieco@uah.es)

<sup>2</sup>CSIRO Land and Water, GPO Box 1666, Canberra ACT 2601, Australia.

[marta.yebra@csiro.au](mailto:marta.yebra@csiro.au)

<sup>3</sup>Departamento de Ingeniería Topográfica, Universidad del País Vasco. Vitoria. Spain.

[aitor.bastarrika@ehu.es](mailto:aitor.bastarrika@ehu.es)

### ABSTRACT

This paper presents an operational algorithm to produce Live Fuel Moisture Content (LFMC) at national scale from MODIS data. The algorithm is based on the inversion of Radiative Transfer Models (RTM) that estimate moisture content based on different simulation scenarios. In addition, logistic regression models were calibrated to convert the derived LFMC values into Ignition Probability (IP) maps. The areas under the curve obtained by the Receiver Operating Characteristic (ROC) plot method provided by the models were close to 0.6. Several statistical analyses were performed in order to ascertain whether the variables proposed to be included in the fire danger model were significantly related to forest fires. A non parametric U-Mann-Withney test confirmed significant differences between fire and non-fire pixels ( $p < 0.001$ ). Fire pixels occurred at significantly lower LFMC values than the non-fire pixels.

Keywords: Live Fuel Moisture Content, Spain, Radiative Transfer Models, Ignition Probability, MODIS.

CONTENIDO DE HUMEDAD DE LA VEGETACIÓN VIVA Y PROBABILIDAD DE IGNICIÓN EN EL TERRITORIO DE LA PENÍNSULA IBÉRICA ESPAÑOLA

### RESUMEN

Se propone un algoritmo para generar una cartografía del contenido de humedad de la vegetación viva (LFMC) de forma operativa. El algoritmo está basado en la inversión de los modelos de transferencia radiativa, basados en distintos escenarios de simulación del contenido de agua. Para convertir los valores de LFMC en mapas de Probabilidad de Ignición (IP), se calibraron modelos de regresión logística. El área bajo la curva obtenida por el método ROC fue próxima a 0,6. Finalmente, se estudió si las variables propuestas en los modelos de peligro de incendio estaban

relacionadas con los incendios forestales de forma significativa. El test no paramétrico de la U-Mann-Whitney confirmó que las variables presentaban diferencias significativas entre los píxeles de incendio y no incendio ( $p < 0,001$ ). Los píxeles con incendio mostraron valores de LFMC significativamente menores que los píxeles sin incendio.

Palabras clave: Contenido de humedad de la vegetación viva, escala nacional, modelos de transferencia radiativa, probabilidad de ignición, MODIS.

## 1. Introduction

Live Fuel Moisture Content (LFMC) is a critical component of forest fire danger estimation, as it is closely related to fire ignition and propagation (Yebra and Chuvieco, 2009). LFMC is computed as:

$$LFMC = \left( \frac{W_w - W_d}{W_d} \right) \times 100 \quad (1)$$

where  $W_w$  is the wet weight and  $W_d$  is the dry weight obtained after oven drying the same sample at 60 °C for 48 h (Viegas *et al.*, 1992).

To date a number of methods have been developed to estimate LFMC, including field work and weather indices. However, those based on Earth Observation data are the most operational, since they cover vast areas with a temporal resolution very adequate to capture the dynamism of the LFMC. Satellite images and both empirical and simulation methods have been employed to retrieve LFMC (Garcia *et al.* 2008; Trombetti *et al.* 2008; Yebra and Chuvieco 2009; Caccamo *et al.*, 2011). Empirical models based on NOAA-AVHRR imagery have been used operationally in Spain (Garcia *et al.*, 2008). Since the models were calibrated and validated for Mediterranean grassland and shrubland they only provided reliable estimates of LFMC in areas with similar vegetation types/species.

Simulation approaches based on Radiative Transfer Models (RTM) have proven to deliver better results to estimate LFMC than empirical methods as they present higher generalization potential (Yebra *et al.*, 2008a; Yebra *et al.*, 2008b). RTM work in forward or backward mode. The forward mode establishes scenarios by assigning input biophysical parameters to simulate expected spectra for different conditions. Both inputs parameters and output spectra are commonly stored in a Look Up Table (LUT). The backward mode compares the simulated spectra and the observed pixel reflectances, assigning to that pixel the input parameters of the most similar simulated spectra. Several inversion methodologies are available for this purpose. The inversion based on the LUT technique is noteworthy (Combal *et al.*, 2002), as it provides a control scenario on the input parameters to be searched for, and allows the identification of ambiguous situations when different sets of input parameters produce similar spectra (Gobron *et al.*, 2000; Saich *et al.*, 2003). The similarity between observed and simulated spectra is measured by a merit function (root mean square error or minimum angle are common choices). To obtain accurate results in the inversion

process it is important to create ecologically based LUTs by means of including ecological information in the parameterizations of the RTM (Yebra and Chuvieco, 2009). Several studies have inverted RTM to retrieve the LFMC of a certain vegetation type (grassland, shrubland and woodland) or region of Spain and different species specific LUTs have been already created. In this sense, Yebra *et al.* (2008b; 2009) estimated LFMC for Mediterranean grassland and shrubland while Jurdao (2012) improved those LUTs to be applicable to the Eurosiberian region. Finally, Jurdao *et al.* (2013) extended the efforts to generate LUTs to be applied in woodland located in both the Eurosiberian and the Mediterranean regions. For the present research, all these previous LUTs generated to resemble different vegetations types and regions of the Peninsular territory of Spain were jointly used to invert RTM and operatively produce LFMC from MODIS reflectance data. The derived LFMC grids were converted into Ignition Probability (IP) based on logistic regression models following the methodology developed by Jurdao *et al.* (2012).

## 2. Methods

### 2.1. Stratification units

The Iberian Peninsular territory of Spain, which covers around 490.000 km<sup>2</sup>, is characterized by its ecological diversity. According to Rivas Martínez (1983), the Iberian Peninsula is stratified in the Mediterranean and the Eurosiberian region. Rainfall ranges from 400-500 mm in the Mediterranean region, while reaches 2000 mm in the Eurosiberian region. In addition, the summer is drier in the former region so the species are highly adapted to drought (e.g. *Quercus ilex* L., *Quercus faginea*, L., etc.). On the other hand, the Eurosiberian region is characterized by more temperate summers and more closed forests, where species such as *Fagus sylvatica* L. may depend on the humidity and the shade as a requisite for survival. Because of these differences, the Mediterranean region can be considered a water-limited environment, whereas the Eurosiberian region is an energy-limited environment (Budiko, 1974). Due to the diverse climatic and ecological characteristics of both regions, a national algorithm should consider this biogeographical stratification. Thus, in order to achieve a national LFMC map, the biogeographical regions should be taken into account as well as the characteristic vegetation types. The second criterion to stratify was based on the vegetation units, following the Spanish Forest Map MFE200 (<http://www.magrama.gob.es/es/biodiversidad/servicios/banco-datos-naturaleza/informacion-disponible/mfe200.aspx>, last accessed January, 2012) which differentiates between grassland, shrubland and woodland (Figure 1). Consequently, for the present study, a total of six stratification units were established: Mediterranean Grassland (MG), Mediterranean Shrubland (MS), Mediterranean Woodland (MW), Eurosiberian Grassland (EG), Eurosiberian Shrubland (ES) and Eurosiberian Woodland (EW).

Jurdao Knecht, S., Yebra Álvarez, M., Bastarrika Izagirre, A., Chuwieco Salinero, E. (2013): "Live fuel moisture content and ignition probability in the Iberian Peninsular territory of Spain", *GeoFocus (Artículos)*, nº 13-2, p. 25-40. ISSN: 1578-5157

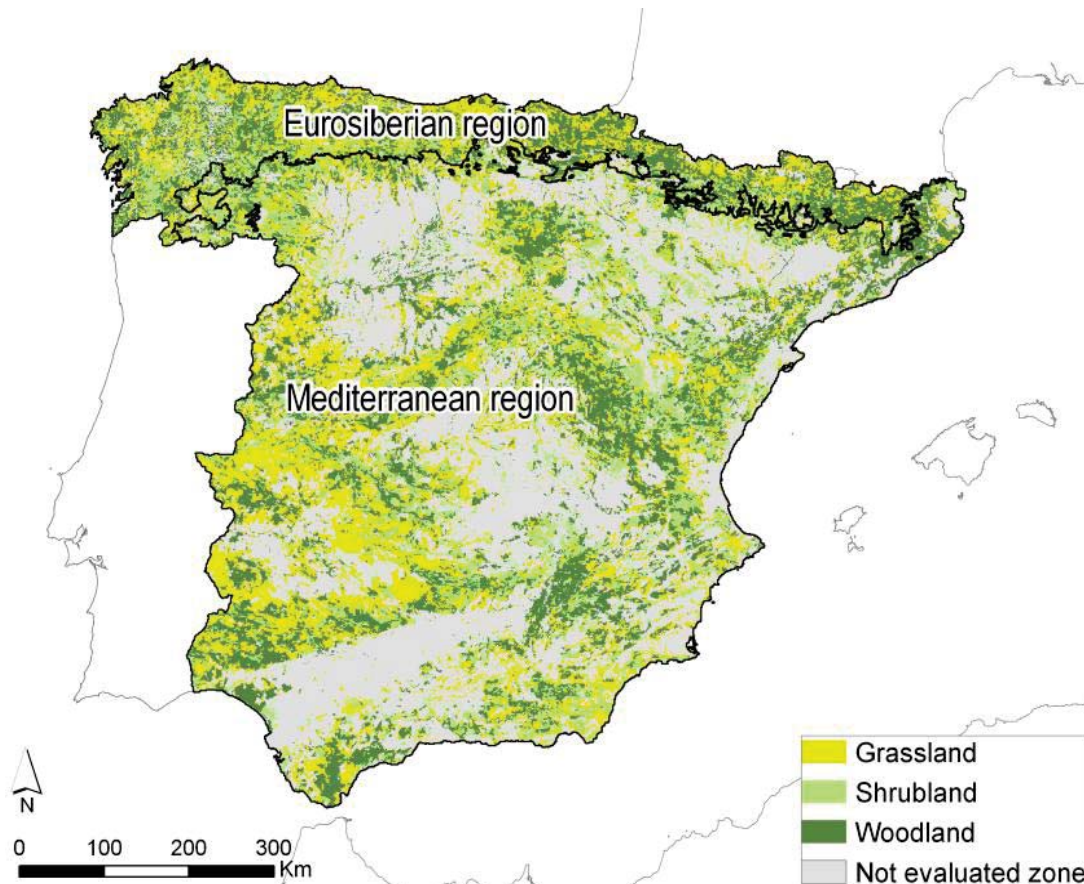


**Figure 1. Biogeographical regions and vegetation types considered to obtain the LFMC cartography.**

## 2.2. Reflectance data

The 500-meter Nadir BRDF-Adjusted reflectance product (MCD43A4) was selected as reflectance input. This MODIS product is a 16-day composite of reflectance, estimated using a bidirectional reflectance distribution function (BRDF) to model the values as if they were taken from the nadir. This significantly reduces noise due to anisotropic scattering effects of surfaces under different illumination and observation conditions (Schaaf *et al.*, 2002). Each composite is computed every 8 days and contains 16 days of data at 500m of spatial resolution from Terra and Aqua satellites. MCD43A4 composites were calculated from daily Terra-Aqua MODIS data received by MODIS reception antenna installed at the University of Oviedo (<http://www.indurot.uniovi.es>, last accessed March, 2012). A description of the reflectance bands is summarized in table 1. In addition to the spectral bands, the Normalized Difference Infrared Index (NDII<sub>6</sub>) was computed (Eq. 2, Hunt and Rock, 1989), as it has been shown closely related to vegetation moisture content.

Jurdao Knecht, S., Yebra Álvarez, M., Bastarrika Izagirre, A., Chuvieco Salinero, E. (2013): "Live fuel moisture content and ignition probability in the Iberian Peninsular territory of Spain", *GeoFocus (Artículos)*, n° 13-2, p. 25-40. ISSN: 1578-5157

$$NDII_6 = \frac{\rho_{NIR} - \rho_{SWIR}}{\rho_{NIR} + \rho_{SWIR}} \quad (2)$$

**Table 1. Characteristics of the MCD43 reflectance bands**

Band	Description	Bandwidth (nm)	Central wavelength (nm)
1	Red	620-670	648
2	NIR	841-876	858
3	Blue	459-479	470
4	Green	545-565	555
5	SWIR	1230-1250	1240
6	SWIR	1628-1652	1640
7	SWIR	2105-2155	2130

### 2.3. LFMC algorithm description

In order to retrieve LFMC, six LUTs (for MG, MS, MW, EG, ES and EW) obtained in previous studies were employed (figure 2).

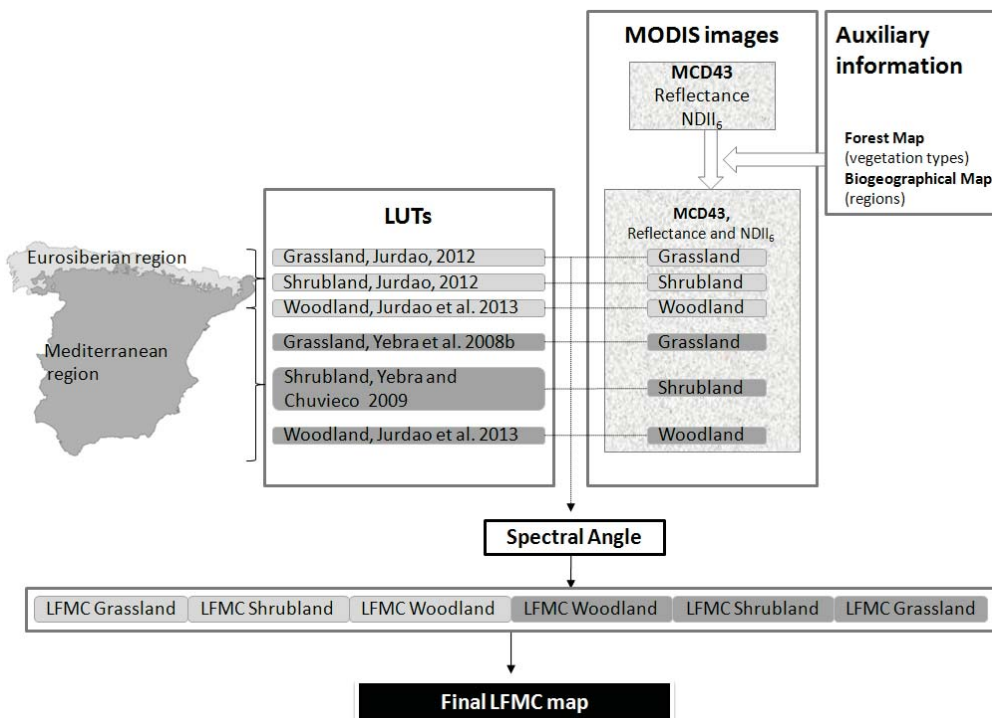


**Figure 2. Overview of the workflow followed to derive the LFMC product.**

### 2.3.1. Reference LUTs description

The production of the LFMC cartography was based on previous work performed by Yebra *et al.* (2008b; 2009) and Jurdao *et al.* (2013) (table 2). The mentioned authors selected at leaf level the PROSPECT model (Jacquemoud, 1990) since more ecological studies measured the biophysical parameters on the units considered by this RTM. At canopy level, the SAILH model (Verhoef, 1984) was selected to obtain, in forward mode, the reference LUTs of grassland and shrubland (Yebra *et al.*, 2008b; Yebra and Chuvieco, 2009; Jurdao, 2012). GeoSail (Huemmrich, 2001) is a geometrical model successfully employed in studies focused on the retrieval of vegetation properties in a wide range of tree species (Kötz *et al.*, 2004; de Santis *et al.*, 2010). Therefore, it was the RTM employed to obtain the reference LUTs of woodlands (Jurdao *et al.*, 2013).

**Table 2. Statistics of the observed LFMC (Obs.) and parameterized LFMC (Param.) per region and vegetation type and the source reference from which the models were taken; Min., minimum; Max., maximum**

				Eurosiberian region		Mediterranean region	
				LFMC (%)	Reference	LFMC (%)	Reference
Vegetation type	Grassland	Obs.	Min.	28.5	(Jurdao 2012)	0.9	(Yebra <i>et al.</i> 2008b)
			Max.	373.6		302.1	
	Param.	Min.	1.3	1.4			
		Max.	309.2	391.7			
	Shrubland	Obs.	Min.	69.9	(Jurdao 2012)	38.9	(Yebra and Chuvieco 2009)
			Max.	205.6		187.0	
Param.	Min.	50.6	44.6				
	Max.	256.9	135.7				
Woodland	Obs.	Min.	73.1	(Jurdao <i>et al.</i> 2013)	15.6	(Jurdao <i>et al.</i> 2013)	
		Max.	251.6		160.5		
Param.	Min.	63.5	20.8				
	Max.	310	169.2				

The authors focused their efforts on the parameterization of RTM for a certain region and vegetation type to achieve reference LUTs specific for those regions/vegetation types. For that, they performed detailed studies to obtain ecological information from literature, laboratory experiments and field campaigns. For the present research, we studied the models already developed and included them in a unique algorithm to obtain operatively relevant national LFMC maps. In general terms, the LUTs presented minimum and maximum LFMC values similar to what it was observed in the field (table 2). The observed LFMC data come from the database developed by the Department of Geography of the University of Alcalá in collaboration with other organizations (Chuvieco *et al.*, 2011).

### 2.3.2. LUT inversion technique

The backward mode or inversion was based on the LUT technique. The merit function in this case was the spectral angle (SA, Eq. 3, Kruse *et al.*, 1993) as it is insensitive to illumination or albedo effects:

$$SA(\vec{v}, \vec{w}) = \cos^{-1} \left( \frac{\vec{v} \times \vec{w}}{\|\vec{v}\| \times \|\vec{w}\|} \right) \quad (3)$$

where  $v$  and  $w$  are the observed (satellite image) and the reference (LUT) spectral respectively, both of them considered as an  $m$ -dimensional feature vector, with  $m$  being the number of spectral channels.

Then, for each pixel, the spectrum of the LUT was selected which was most similar (with minimum SA) to that contained on the target pixel and the corresponding LFMC value was assigned to it. As LFMC is not an input parameter considered in the simulation models, it was obtained by the ratio between two of the RTM input parameters (Eq. 4).

$$LFMC = \frac{EWT}{DMC} \quad (4)$$

where EWT is the Equivalent Water Thickness (Eq. 5) and DMC is the Dry Matter Content (Eq. 6).

$$EWT = \frac{W_w - W_d}{leafArea} \quad (5)$$

$$DMC = \frac{W_d}{leafArea} \quad (6)$$

As a result, an LFMC map was obtained. To make this process operative, a routine was programmed in Interactive Data Language (IDL).

### 2.3.3. Accuracy assessment

In order to offer the accuracy of the estimates in the different regions/vegetation types, the Root Mean Square Error (RMSE, Eq. 7) computed between the estimated LFMC values given by the models, and the observed LFMC in the field was taken from previous studies and shown in table 3. The validation sites were distributed covering the whole national territory (Chuvieco *et al.*, 2011).

$$RMSE = \sqrt{\frac{\sum_{i=1}^n (LFMC_{i,obs} - LFMC_{i,est})^2}{n}} \quad (7)$$

where  $LFMC_{i,obs}$  and  $LFMC_{i,est}$  are the observed and the estimated LFMC respectively, and  $n$  is the number of observations.

In addition, it is shown the systematic and the unsystematic portions (RMSEs and RMSEu, respectively). The RMSEs provides a quantitative measurement of the error caused by the model performance and its predictors. On the other side, the RMSEu offers information about the error caused by uncontrolled factors. An adequate model is considered to have an RMSEu higher than the RMSEs as the model estimates errors should be random.

**Table 3. Accuracy of the simulation models used given by the Root Mean Square Error (RMSE), the systematic RMSE (RMSEs) and the unsystematic RMSE (RMSEu)**

		LFMC (%)	RMSE (%)	RMSEs (%)	RMSEu (%)	
Vegetation type	Grassland	Eurosiberian All	41.9	12.6	39.9	
		Eurosiberian <200	30.6	3.6	30.4	
		Mediterranean	24.6	8.7	22.9	
	Shrubland	Eurosiberian		19.3	10.6	16.1
		Mediterranean		19.8	9.5	17.3
	Woodland	Eurosiberian		28.7	12.8	28.8
Mediterranean			27.3	15.4	22.6	

The RMSE provided by the models was around 40 % for the Eurosiberian grassland (Jurdao, 2012). However, due to the fact that the Eurosiberian grassland is affected by the dew which increases the observed LFMC values above 200 %, the accuracy is also given below the threshold of LFMC equal to 200 %. With this adjustment, the RMSE was reduced to 30.6 % (Table 3). The Mediterranean grassland presented a RMSE around 25 % (Yebra *et al.*, 2008b). For shrubland, the RMSE was below 20 % for the Eurosiberian and the Mediterranean regions (Yebra and Chuvieco 2009; Jurdao 2012). Finally, the woodland vegetation type offered the highest RMSE (RMSE<30 %, (Jurdao *et al.*, 2013).

#### 2.4. Conversion of LFMC into IP

There are many methodological approaches to derive IP from LFMC. Some of them are based on biophysical parameters derived from experiment results (Chuvieco *et al.*, 2004; Dimitrakopoulos *et al.*, 2010) while others relate moisture values to fire occurrence (Andrews *et al.*, 2003; Dennison and Moritz, 2009). In Spain, within the first group, Chuvieco *et al.*(2004) presented a method based on the inverse linear relation between the moisture of extinction (a biophysical parameter defined as the moisture thresh- old above which fire cannot be sustained) and the actual LFMC value (the closer to the ME; the lower the IP). Within the last group, López *et al.* (1991) and González-Alonso *et al.* (1997) obtained the IP basing part of their methodologies on the temporal evolution of the Normalized Difference Vegetation Index (NDVI) as they assumed that the IP increased when the NDVI decreased, since this phenomenon may be linked to an increase in water stress. More recently, logistic regression (LR) models were used to estimate IP (Chuvieco *et al.*, 2009; Jurdao *et al.*, 2012). Particularly, the last authors related seven years of fire occurrence (2001-2007) to the LFMC derived from NOAA-AVHRR (Jurdao *et al.*, 2012). Fire occurrence was based



on the standard MODIS Thermal Anomalies product (MOD14, Giglio *et al.*, 2003) while the LFMC data was computed according to Garcia *et al.* (2008) for grassland and shrubland. This product was based on 8-day composites at 1 km<sup>2</sup> spatial resolution. Three methods were tested in order to derive IP from LFMC: histograms and percentiles, classification trees and logistic regression (LR). LR provided the most satisfactory results (the Areas Under the Curve, AUC, obtained by the Receiver Operating Characteristic plot method, ROC, were 0.62 and ≈0.7 for grassland and shrubland respectively (Jurdao *et al.*, 2012). The variables included to model IP were: (1) the LFMC corresponding to the 8-day period prior to the period including the fire date (LFMC<sub>t-1</sub>); (2) the LFMC corresponding to the 8-day period prior to LFMC<sub>t-1</sub> (LFMC<sub>t-2</sub>); (3) the moisture variation between two previous periods to the fire date (difference); (4) the moisture gradient between the maximum LFMC value and the LFMC of the period before the fire date (slope); and (5) the departure of LFMC values before the fire date from the average value of that period during the time series (anomaly). The 8-day period including the date of the fire (LFMC<sub>t</sub>) was not considered, as the aim was to obtain predictive models. A total of six models (two for the regions and four which considered a different region/vegetation type combination) were obtained (Jurdao *et al.*, 2012).

For the present study, as a preliminary attempt to derive IP from LFMC based on MODIS images, we developed a similar methodology as Jurdao *et al.* (2012) based on LR but applied only to the specific regions. As no distinction among vegetation types was made, just two models were obtained (Mediterranean and Eurosiberian models). For that, it was necessary to develop a database with fire pixels and non-fire pixels. The MODIS hot spots product derived from EFFIS for the years 2010 and 2011 (detected by both TERRA and AQUA satellites) was selected as a reference of fire occurrence. This is a filtered product based on the MODIS Rapid Response System hotspot detection, focused on minimizing false alarms and filter out active fires not qualified as wildfires (e.g. agricultural burnings) (<http://effis.jrc.ec.europa.eu/about/technical-background/active-fire-detection>, last accessed May, 2012).

Following Jurdao *et al.* (2012), the unburned pixels were randomly distributed 10 Km distant from the fire pixels, to avoid selecting unburned pixels contaminated by actual burns, but not further than 20 km to keep the same ecological characteristics of the vegetation of the areas affected by fires (2012). Afterwards, the LFMC<sub>t-1</sub>, the LFMC<sub>t-2</sub>, the difference and the slope values were extracted for all the fire and non-fire pixels. The variable Anomaly was not considered as its calculation requires a large time series of data and the LFMC derived from MODIS data has been processed up to now only for the years 2010 and 2011. The independent variables were entered in the model, resulting in a linear equation (Eq. 8). Then, the equation was included in the computation of IP (Eq. 9), which stands for the probability of fire.

$$z = \beta_0 + \beta_1 x_1 + \beta_2 x_2 + \dots + \beta_r x_r \quad (8)$$

$$IP = \left( \frac{1}{1 + e^{-z}} \right) \quad (9)$$

Afterwards, the results of the LR models were assessed using the AUCs obtained by the ROC plot method (Fielding and Bell, 1997).

Finally, the non-parametric U-Mann-Whitney test for differences was used to test whether the four explanatory variables showed statistical significance between fire and non-fire pixels. In addition, the same test was applied to ascertain if there were significant differences in the annual median and the annual mean between fire and non-fire pixels, so these values also needed to be extracted in the same way as the explanatory variables. Additionally, a study was made to determine whether the LFMC was lower in places with fires than where non fires were encountered, by means of the box-plots computation.

### 3. Results and discussion

#### 3.1. LFMC

The national LFMC maps showed the temporal trends of LFMC (figure 3). At the beginning of May, LFMC reached values higher than 140 % in most of the Iberian Peninsula (figure 3a). Lower LFMC values were encountered in the south-east, close to the Mediterranean coast. At the end of May, the lower LFMC values increased mainly in areas occupied by grasslands (figure 3b). In June, a decrease in LFMC is clearly observed, since areas with previous LFMC between 105-140 % registered LFMC values below 105 % (figure 3c). Other areas with previous LFMC between 70-105 % registered LFMC values below 70 % and so on. The LFMC detriment was accentuated in August (figure 3d) which continued until the beginning of October (figure 3e). Finally, in November, it was noted that the LFMC started to increase (figure 3f).

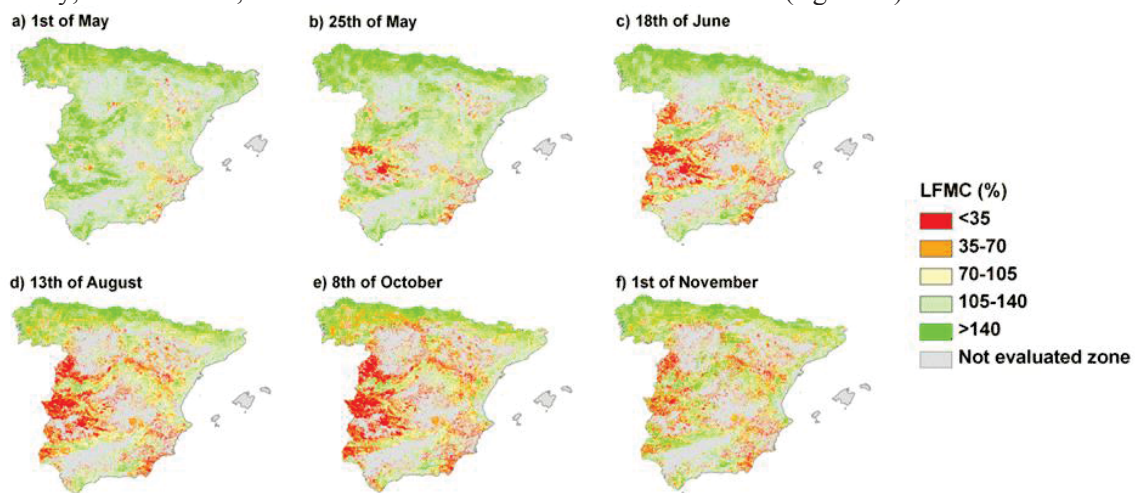


**Figure 3. LFMC for 2011 at 500 m resolution.**

The temporal trends can also be observed in figure 4. In addition, this figure shows the LFMC variability in the different vegetation types and regions under consideration. Woodlands present the lowest variability (LFMC between 70 % and 150 %, approximately), then shrublands (LFMC between 50 % and 150 %, approximately) and finally the grassland vegetation type show

the highest variability (LFMC between 30 % and 300 %, approximately). It is remarkable that higher LFMC variability is showed in the Eurosiberian region rather than in the Mediterranean region since, in the former region, higher LFMC are reached. The 25<sup>th</sup> of May, the Eurosiberian grassland presented LFMC values around 300%, possibly owing to the dew that characterized this region, especially in spring.

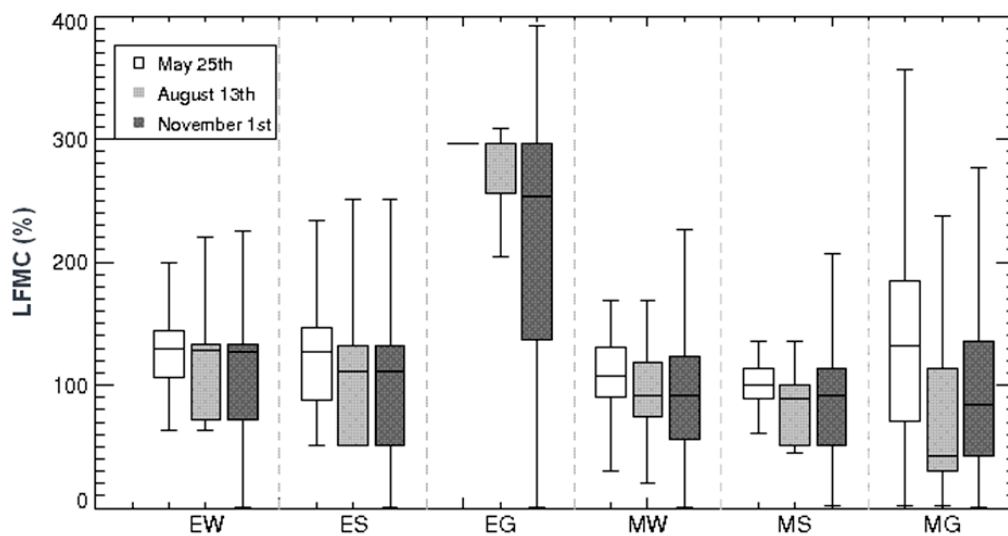


**Figure 4. Estimated LFMC values for the vegetation types and regions considered in three specific dates. EW: Eurosiberian Woodland; ES: Eurosiberian Shrubland; EG: Eurosiberian Grassland; MW: Mediterranean Woodland; MS: Mediterranean Shrubland; MG: Mediterranean Grassland.**

### 3.2. IP

The resulting variables included in the equations to model IP were the LFMC<sub>t-1</sub> for the Eurosiberian region (Eq. 10), and the difference for the Mediterranean region (Eq. 11). However, the models were less accurate (AUCs= 0.6 and 0.57 for the Eurosiberian and Mediterranean region respectively) than the models obtain by Jurdao *et al.* (2012) (AUCs > 0.6). This is probably due to the fact that we only considered two years for the calibration whereas Jurdao *et al.*, (2012) considered seven years.

$$z = (-0.003 \times LFMC_{t-1}) + 0.602 \quad (10)$$

$$z = (0.006 \times difference) - 0.192 \quad (11)$$

As an example, we included both equations in the computation of IP for the 13<sup>th</sup> of August 2011 (figure 5). The LFMC<sub>t-1</sub> was taken from the LFMC composite calculated one week before (the 13<sup>th</sup> of August 2011) and the difference was computed with the LFMC one and two weeks before (the 13<sup>th</sup> of August 2011 and the 5<sup>th</sup> of August 2011).

Jurdao Knecht, S., Yebra Álvarez, M., Bastarrika Izagirre, A., Chuwieco Salinero, E. (2013): "Live fuel moisture content and ignition probability in the Iberian Peninsular territory of Spain", *GeoFocus (Artículos)*, nº 13-2, p. 25-40. ISSN: 1578-5157

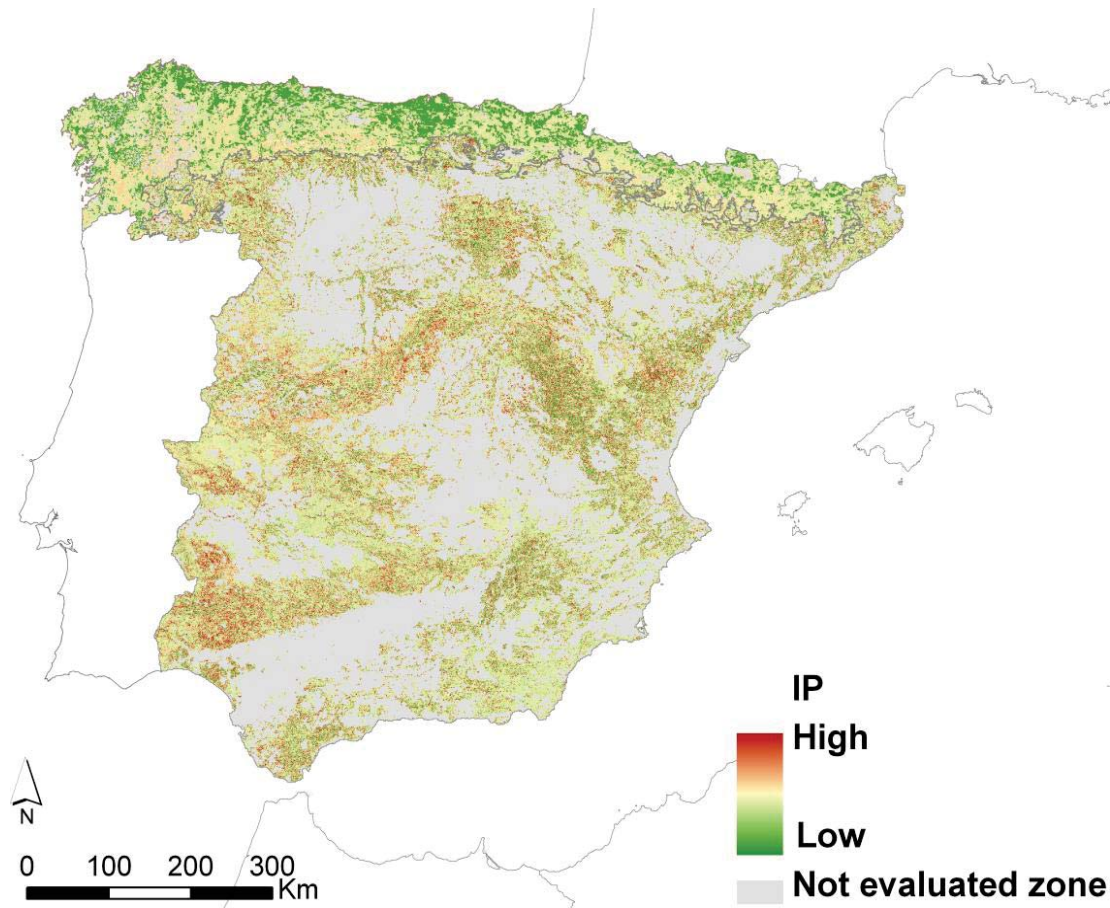
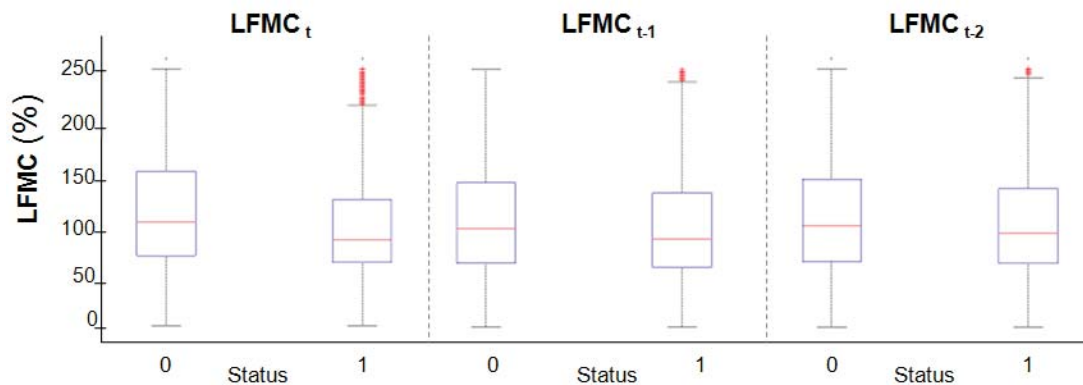


Figure 5. IP estimated for the 21<sup>st</sup> of August 2011.

Significant differences were found between fire and non-fire pixels for all the analyzed variables (table 4, p-values<0.001). In addition, according to the box-plots, it was observed that the moisture level was lower in the fire pixels than in the non-fire pixels and that the moisture level one and two weeks prior to the fire was also lower in the fire pixels (figure 6). Hence, it was demonstrated that, in general terms, fires occur under lower LFMC conditions. Taking into account that the LFMC prior to the fire (LFMC  $t_{-1}$  and LFMC  $t_{-2}$ ) was also lower for the fire pixels, its usefulness as a fire predictor variable was demonstrated.

Table 4. U-Mann-Whitney z value and significant level found between fire and non-fire pixels for several variables

	LFMC $t$	LFMC $t_{-1}$	LFMC $t_{-2}$	Difference	Slope	Anual Median	Anual Mean
z	-13.93	-6.98	-5.70	-4.80	-4.56	-8.69	-8.707
p-value	<0.001	<0.001	<0.001	<0.001	<0.001	<0.001	<0.001



**Figure 6. Box-plot result for the variables  $LFMC_t$ ,  $LFMC_{t-1}$  and  $LFMC_{t-2}$ . Status=0: non-fire pixels; Status=1: fire pixels.**

#### 4. Conclusions

We provide an operative method to retrieve LFMC and IP for the Iberian Peninsular territory of Spain based on MODIS images and the inversion of RTM. Previous studies have aimed similar goals based on empirical fittings between field data and NOAA images. Our method relies on specific simulation models developed for Eurosiberian and Mediterranean regions of Spain, covering the three main vegetation units (Woodlands, Shrublands and Grasslands). The model of ignition probability based on logistic regression analysis of LFMC values, did not provide enough accuracy for the time being (AUCs  $\approx 0.6$ ). It was possibly due to the fact that only two years of analysis were considered (2010-2011). Hence, future research will be focused on extending the LFMC time series in order to achieve more accurate IP models. Finally, we found a strong relationship between LFMC and forest fires as, in general terms, the fire pixels corresponded to pixels with lower LFMC before the fire detection than the non-fire pixels. However, non-fire pixels were found with low LFMC values due to the fact that an ignition source is required to start a fire. Therefore, certain areas with a high potential of being burned (with minimum LFMC values) may not burn because of the lack of an ignition source.

#### Acknowledgments

This research has been funded by the Spanish Ministry of Education and Science by means of the FPU grant program which supports Sara Jurdao, and supported by the FIREGLOBE project (CGL2008-01083), funded by the Spanish Ministry of Science and Technology. We thank the Indurot Institute (University of Oviedo) for their assistance with the MODIS images and Juan Pablo Guerschman (CSIRO Land and Water, Canberra, Australia) for providing assistance with IDL programming.

Jurdao Knecht, S., Yebra Álvarez, M., Bastarrika Izagirre, A., Chuvieco Salinero, E. (2013): "Live fuel moisture content and ignition probability in the Iberian Peninsular territory of Spain", *GeoFocus (Artículos)*, nº 13-2, p. 25-40. ISSN: 1578-5157

---

## References

- Andrews, P. L., D. O. Loftsgaarden y L. S. Bradshaw (2003): "Evaluation of fire danger rating indexes using logistic regression and percentile analysis", *International Journal of Wildland Fire*, 12, pp. 213-226.
- Budiko, M. I. (1974): *Climate and Life*. New York, Academic Press.
- Caccamo, G., L. A., Chisholm, R. A., Bradstock y M. L. Puotinen (2011): "Assessing the sensitivity of MODIS to monitor drought in high biomass ecosystems", *Remote Sensing of Environment*, 115, 20, pp. 2626-2639.
- Chuvieco, E., I. Aguado y A. Dimitrakopoulos (2004): "Conversion of fuel moisture content values to ignition potential for integrated fire danger assessment", *Canadian Journal of Forest Research-Revue Canadienne de Recherche Forestiere*, 34, 11, pp. 2284-2293.
- Chuvieco, E., I. González, F. Verdú, I. Aguado y M. Yebra (2009): "Prediction of fire occurrence from live fuel moisture content measurements in a Mediterranean ecosystem", *International Journal of Wildland Fire*, 18, pp. 430-441.
- Chuvieco, E., M. Yebra, S. Jurdao, I. Aguado, J. Salas, M. García, H. Nieto, A. de Santis, D. Cocero, D. Riaño, S. Martínez, E. Zapico, C. Recondo, J. Martínez-Vega, M. P. Martín, J. Riva, F. Pérez y F. Rodríguez-Silva (2011): "Field fuel moisture measurements on Spanish study sites. Department of Geography, University of Alcalá." [http://www.geogra.uah.es/emilio/FMC\\_UAH.html](http://www.geogra.uah.es/emilio/FMC_UAH.html).
- Combal, B., F., Baret, M., Weiss, A., Trubuil, D. Mace, A. Pragne`re, R. Myneni, Y. Knyazikhin y L. Wang (2002): "Retrieval of canopy biophysical variables from bidirectional reflectance Using prior information to solve the ill-posed inverse problem", *Remote Sensing of Environment*, 84, pp. 1-15.
- Crapper, P. F. y K. C. Hynson (1983): "Change detection using Landsat photographic imagery", *Remote Sensing of Environment*, 13, pp. 291-300.
- de Santis, A., G. P. Asner, P. J. Vaughan y D. E. Knapp (2010): "Mapping burn severity and burning efficiency in California using simulation models and Landsat imagery", *Remote Sensing of Environment*, 114, 7.
- Dennison, P. E. y M. A. Moritz (2009): "Critical live fuel moisture in chaparral ecosystems: a threshold for fire activity and its relationship to antecedent precipitation", *International Journal of Wildland Fire*, 18, pp. 1021-1027.
- Dimitrakopoulos, A. P., I. D. Mitsopoulos y K. Gatoulas (2010): "Assessing ignition probability and moisture of extinction in a Mediterranean grass fuel", *International Journal of Wildland Fire*, 19, pp. 29-34.
- Fielding, A. H. y J. F. Bell (1997): "A review of methods for the assessment of prediction errors in conservation presence/absence models", *Environmental Conservation*, 24, pp. 38-49.

Jurdao Knecht, S., Yebra Álvarez, M., Bastarrika Izagirre, A., Chuvieco Salinero, E. (2013): "Live fuel moisture content and ignition probability in the Iberian Peninsular territory of Spain", *GeoFocus (Artículos)*, n° 13-2, p. 25-40. ISSN: 1578-5157

---

García, M., I. Aguado y E. Chuvieco (2008): "Combining AVHRR and meteorological data for estimating live fuel moisture content in forest fire danger rating", *Remote Sensing of Environment*, 112, pp. 3618-3627.

Giglio, L., J. Descloitres, C. O. Justice y J. B. Kauffmann (2003): "An Enhanced Contextual Fire Detection Algorithm for MODIS", *Remote Sensing of Environment*, 87, pp. 273-282.

Gobron, N., B. Pinty, M. M. Verstraete, J. V. Martonchik, Y. Knyazikhin y D. J. Diner (2000): "Potential of multiangular spectral measurements to characterize land surfaces: Conceptual approach and exploratory application", *Journal of Geophysical Research*, 105, D13, pp. 17539-17549.

González-Alonso, F., J. M. Cuevas, J. L., Casanova, A. Calle y P. Illera (1997): "A forest fire risk assessment using NOAA-AVHRR images in the Valencia area, Eastern Spain", *International Journal of Remote Sensing*, 18, pp. 2201-2207.

Huemmerich, K. F. (2001): "The GeoSail model: a simple addition to the SAIL model to describe discontinuous canopy reflectance", *Remote Sensing of Environment*, 75, pp. 423-431.

Hunt, E. R. y B. N. Rock (1989): "Detection of changes in leaf water content using near and middle-infrared reflectances", *Remote Sensing of Environment*, 30, pp. 43-54.

Jacquemoud, S. (1990): "PROSPECT: a model to leaf optical properties spectra", *Remote Sensing of Environment*, 34, pp. 74-91.

Jurdao, S. (2012): "Remotely sensed Live Fuel Moisture retrieval using Radiative Transfer Models", *Geography*, Alcalá de Henares, Alcalá University, 168.

Jurdao, S., E. Chuvieco y J. M. Arevalillo (2012): "Modelling fire ignition probability from satellite estimates of live fuel moisture content", *Fire Ecology*, 8, 1, pp. 77-97.

Jurdao, S., M. Yebra, E. Chuvieco y J. P. Guerschman (2013): "Regional estimation of woodland moisture content by inverting Radiative Transfer Models", *Remote Sensing of Environment*, 132, pp. 59-70.

Kötz, B., M. Schaepman, F. Morsdorf, P. Bowyer, K. Itten y B. Allgöwer (2004): "Radiative transfer modeling within a heterogeneous canopy for estimation of forest fire fuel properties", *Remote Sensing of Environment*, 92, pp. 332-344.

Kruse, F. A., A. B. Lefkoff, J. B. Boardman, K. B. Heidebrecht, A. T. Shapiro, P. J. Barloon y A. F. H. Goetz (1993): "The Spectral Image Processing (SIPS) - Interactive Visualization and Analysis of Imaging Spectrometer Data", *Remote Sensing of Environment*, 44, pp. 145-163.

López, S., F. González, R. Llop y J. M. Cuevas (1991): "An evaluation of the utility of NOAA AVHRR images for monitoring forest fire risk in Spain", *International Journal of Remote Sensing*, 12, 9, pp. 1841-1851.

Saich, P., P. Lewis y M. I. Disney (2003): "Biophysical parameter retrieval from forest and crop canopies in the optical and microwave domains using 3D models of canopy structure", *Geoscience and Remote Sensing Symposium, IGARSS '03*, Toulouse, IEEE International.

Jurdao Knecht, S., Yebra Álvarez, M., Bastarrika Izagirre, A., Chuvieco Salinero, E. (2013): "Live fuel moisture content and ignition probability in the Iberian Peninsular territory of Spain", *GeoFocus (Artículos)*, nº 13-2, p. 25-40. ISSN: 1578-5157

---

Schaaf, C. B., F. Gao, A. H. Strahler, W. Lucht, X. Li, T. Tsang, N. C. Strugnell, X. Zhang, Y. Jin, J.-P. Muller, P. Lewis, M. Barnsley, P. Hobson, M. Disney, G. Roberts, M. Dunderdale, C. Doll, R. P. d'Entremont, B. Hug, S. Liang, J. L. Privette y D. Roy (2002): "First operational BRDF, albedo nadir reflectance products from MODIS", *Remote Sensing of Environment*, 83, pp. 135-148.

Trombetti, M., D. Riano, M. A. Rubio, Y. B. Cheng y S. L. Ustin (2008): "Multi-temporal vegetation canopy water content retrieval and interpretation using artificial neural networks for the continental USA", *Remote Sensing of Environment*, 112, pp. 203-215.

Verhoef, W. (1984): "Light scattering by leaf layers with application to canopy reflectance modeling: the SAIL model", *Remote Sensing of Environment*, 16, pp. 125-141.

Viegas, D. X., T. P. Viegas y A. D. Ferreira (1992): "Moisture content of fine forest fuels and fire occurrence in central Portugal", *The International Journal of Wildland Fire*, 2, 2, pp. 69-85.

Yebra, M. y E. Chuvieco (2009): "Linking ecological information and radiative transfer models to estimate fuel moisture content in the Mediterranean region of Spain: Solving the ill-posed inverse problem", *Remote Sensing of Environment*, 113, pp. 2403-2411.

Yebra, M., E. Chuvieco y I. Aguado (2008a): "Comparación de modelos empíricos y de transferencia radiativa para estimar contenido de humedad en pastizales: Poder de generalización", *Revista de Teledetección*, 29, pp. 73-90.

Yebra, M., E. Chuvieco y D. Riaño (2008b): "Estimation of live fuel moisture content from MODIS images for fire risk assessment", *Agricultural and Forest Meteorology*, 148, 4, pp. 523-536.